

Cu^{II}-Azide Polymers of Cu₃ and Cu₆ Building Units: Synthesis, Structures, and Magnetic Exchange Mechanism[†]

Sandip Mukherjee, Bappaditya Gole, Rajesh Chakrabarty, and Partha Sarathi Mukherjee*

Department of Inorganic and Physical Chemistry, Indian Institute of Science, Bangalore-560012, India

Received September 18, 2009

Two new neutral copper-azido polymers [Cu₃(N₃)₆(tmen)₂]_n (**1**) and [Cu₆(N₃)₁₂(deen)₂]_n (**2**) [tmen = *N,N,N',N'*-tetramethylethylenediamine and deen = *N,N*-diethylethylenediamine] have been synthesized by using lower molar equivalents of the chelating diamine ligands with Cu(NO₃)₂·3H₂O and an excess of NaN₃. The single crystal X-ray structure shows that in the basic unit of the 1D complex **1**, the three Cu^{II} ions are linked by double end-on azido bridges with Cu–N_{EO}–Cu angles on both sides of the magnetic exchange critical angle of 108°. Complex **2** is a 3D framework of a basic Cu₆ cluster. Cryomagnetic susceptibility measurements over a wide range of temperature exhibit dominant ferromagnetic behavior in both the complexes. Density functional theory calculations (B3LYP functional) have been performed on the trinuclear unit to provide a qualitative theoretical interpretation of the overall ferromagnetic behavior shown by the complex **1**.

Introduction

Extended coordination networks and discrete polynuclear clusters of paramagnetic metal ions held close together by short bridging ligands have received considerable attention in the field of molecular magnetism in the past two decades.¹ These materials have also offered opportunities to probe the fundamental magnetic phenomena, such as long-range ordering, spin canting, metamagnetism, anisotropy, relaxation dynamics, and quantum tunneling of magnetization, both

experimentally and theoretically.² The diversities of molecular-magnetic materials in structure and magnetism have been

[†] This work is dedicated to Prof. Richard E. P. Winpenny.

*To whom correspondence should be addressed. E-mail: psm@ipc.iisc.ernet.in. Fax: 91-80-23601552. Phone: 91-80-22933352.

(1) (a) Stamatatos, T. C.; Christou, A. G.; Jones, C. M.; O'Callaghan, B. J.; Abboud, K. A.; O'Brien, T. A.; Christou, G. *J. Am. Chem. Soc.* **2007**, *129*, 9840. (b) Bagai, R.; Abboud, K. A.; Christou, G. *Inorg. Chem.* **2007**, *46*, 5567. (c) Vittal, J. J. *Coord. Chem. Rev.* **2007**, *251*, 1781. (d) Yoon, J.; Solomon, E. I. *Coord. Chem. Rev.* **2007**, *251*, 379. (e) Lee, C. F.; Leigh, D. A.; Pritchard, R. G.; Schults, D.; Teat, S. J.; Timco, G. A.; Winpenny, R. E. P. *Nature* **2009**, *458*, 314. (f) Winpenny, R. E. P. *Angew. Chem., Int. Ed.* **2008**, *47*, 7992. (g) Winpenny, R. E. P. *Dalton Trans.* **2002**, *1*. (h) Chandrasekhar, V.; Murugesapandian, B. *Acc. Chem. Res.* **2009**, *42*, 1047. (i) Chandrasekhar, V.; Murugesapandian, B.; Vittal, J. J. *Inorg. Chem.* **2009**, *48*, 1148.

(2) (a) Gatteschi, D.; Sessoli, R. *Angew. Chem.* **2003**, *115*, 278; *Angew. Chem., Int. Ed.* **2003**, *42*, 268. (b) Aromi, G.; Brechin, E. K. *Struct. Bonding (Berlin)* **2006**, *122*, 1. (c) Coulon, C.; Miyasaka, H.; Clérac, R. *Struct. Bonding (Berlin)* **2006**, *122*, 163.

(3) (a) Papaefstathiou, G. S.; Perlepes, S. P.; Escuer, A.; Vicente, R.; Font-Bardía, M.; Solans, X. *Angew. Chem., Int. Ed.* **2001**, *40*, 884. (b) Papaefstathiou, G. S.; Escuer, A.; Vicente, R.; Font-Bardía, M.; Solans, X.; Perlepes, S. P. *Chem. Commun.* **2001**, 2414. (c) Boudalis, A. K.; Donnadieu, B.; Nastopoulos, V.; Clemente-Juan, J. M.; Mari, A.; Sanakis, Y.; Tchuagues, J. P.; Perlepes, S. P. *Angew. Chem., Int. Ed.* **2004**, *43*, 2266. (d) Nanda, P. K.; Aromi, G.; Ray, D. *Inorg. Chem.* **2006**, *45*, 3143. (e) Mandal, D.; Bertolasi, V.; Ribas-Ariño, J.; Ray, D. *Inorg. Chem.* **2008**, *47*, 3465. (f) Mukherjee, P.; Drew, M. G. B.; Garcia, C. J.; Ghosh, A. *Inorg. Chem.* **2009**, *48*, 848. (g) Chattapadhyay, S.; Drew, M. G. B.; Diaz, C.; Ghosh, A. *Inorg. Chem.* **2007**, 2492.

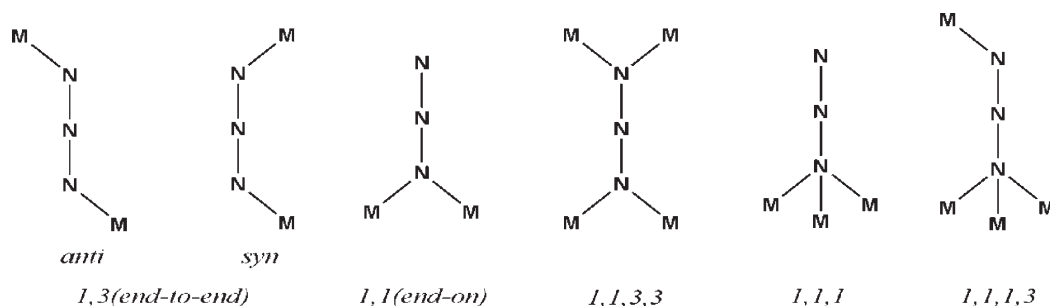
(4) Guo, G.-C.; Mak, T. C. W. *Angew. Chem., Int. Ed.* **1998**, *37*, 3268.

(5) (a) Ribas, J.; Escuer, A.; Monfort, M.; Vicente, R.; Cortes, R.; Lezama, L.; Rojo, T. *Coord. Chem. Rev.* **1999**, *193–195*, 1027 and references therein.

(6) (a) Kahn, O. *Chem. Phys. Lett.* **1997**, *265*, 165. (b) Aubin, S. M. J.; Bolcar, M. A.; Christou, G.; Eppley, H. J.; Foltling, K.; Hendrickson, D. N.; Huffman, J. C.; Squire, R. C.; Tsai, H. L.; Wang, S.; Wemple, M. W. *Polyhedron* **1998**, *17*, 3005. (c) Thomas, L.; Lionti, F.; Ballou, R.; Gatteschi, D.; Sessoli, R.; Barbara, B. *Nature* **1996**, *383*, 145. (d) *Magnetic Molecular Materials*; Gatteschi, D.; Kahn, O.; Müller, J. S.; Palacio, F., Eds.; Kluwer Academic: Dordrecht, The Netherlands, 1991. (e) Sessoli, R.; Tsai, H.-L.; Schake, A. R.; Wang, S.; Vincent, J. B.; Foltling, K.; Gatteschi, D.; Christou, G.; Hendrickson, D. N. *J. Am. Chem. Soc.* **1993**, *115*, 1804. (f) Ouellette, W.; Galan-Mascaros, J. R.; Dunbar, K. R.; Jubieta, J. *Inorg. Chem.* **2006**, *45*, 1909. (g) Shatruk, M.; Dragulescu, A. A.; Chambers, K. E.; Stoian, S. A.; Bominaar, F. A.; Achim, C.; Dunbar, K. R. *J. Am. Chem. Soc.* **2007**, *129*, 6104. (h) Konar, S.; Zangrando, E.; Drew, M. G. B.; Mallah, T.; Ribas, J.; Ray Chaudhuri, N. *Inorg. Chem.* **2003**, *42*, 5966. (i) Tabellion, F. M.; Seidel, S. R.; Arif, A. M.; Stang, P. J. *J. Am. Chem. Soc.* **2001**, *123*, 11982. (j) Tolis, E. I.; Helliwell, M.; Langley, S.; Raftery, J.; Winpenny, R. E. P. *Angew. Chem., Int. Ed.* **2003**, *42*, 3804. (n) Ribas, J.; Escuer, A.; Monfort, Vicente, R.; Cortés, R.; Lezama, L.; Rojo, T. *Coord. Chem. Rev.* **1999**, *193–195*, 1027 and references therein. (o) Kato, M.; Muto, Y. *Coord. Chem. Rev.* **1988**, *92*, 45. (p) Maji, T. K.; Mukherjee, P. S.; Mostafa, G.; Mallah, T.; Cano-Boquera, J.; Chaudhuri, N. R. *Chem. Commun.* **2001**, 1012.

(7) (a) Mondal, K. C.; Song, Y.; Mukherjee, P. S. *Inorg. Chem.* **2007**, *46*, 9736. (b) Price, D. J.; Murry, K. S. *Chem. Commun.* **2002**, 762. (c) Konar, S.; Zangrando, E.; Drew, M. G. B.; Mallah, T.; Ray Chaudhuri, N. *Inorg. Chem.* **2003**, *42*, 5966. (d) Maji, T. K.; Mostafa, G.; Mallah, T.; Boquera, J. C.; Ray Chaudhuri, N. *Chem. Commun.* **2001**, 1012. (e) Sessoli, R.; Gatteschi, D.; Caneschi, A.; Novak, M. A. *Nature* **1993**, *365*, 141. (f) Wernsdorfer, W.; Aliaga-Alcalde, N.; Hendrickson, D. N.; Christou, G. *Nature* **2002**, *416*, 406. (g) Müller, A.; Meyer, J.; Krickemeyer, E.; Beugholt, C.; Bögge, H.; Peters, F.; Schmidtmann, M.; Kögerler, P.; Koop, M. J. *Chem.—Eur. J.* **1998**, *4*, 1000. (h) Leibel, G.; Demeshko, S.; Bauer-Siebenlist, B.; Meyer, F.; Pritzkow, H. *Eur. J. Inorg. Chem.* **2004**, 2413. (i) Demeshko, S.; Leibel, G.; Dechert, S.; Meyer, F. *Dalton Trans.* **2006**, 3458.

Scheme 1. Common Bridging Modes of the Azido Ligand



well illustrated by metal-azido systems for the last two decades.^{3–18}

The azido anion (N_3^-) still remains a popular choice in the field of molecular magnetism as a bridging ligand (Scheme 1) because of its ability to couple metal ions ferromagnetically under suitable conditions. From the structural point of view, it is also very useful to design extended polynuclear complexes, as it can bind up to three metal ions when acting as a monatomic bridge (end-on, EO)³ and up to six using the two terminal nitrogen atoms to bridge (end-to-end, EE).^{4,5} With a very few exceptions, the EE-azido mode generally transmits antiferromagnetic interaction. In this regard, the behavior of the EO-azido mode is very complex.^{6–13} The Cu^{II} azido systems have been most widely studied, and it is now well established that the nature of magnetic exchange in EO-bridged Cu-azido complexes is strongly influenced by the $\text{Cu}-\text{N}_{\text{EO}}-\text{Cu}$ angle. The magnetic interaction between the Cu^{II} ions is ferromagnetic if this angle is below the critical angle of 108° and antiferromagnetic above it.¹⁴ Enhancement of the bulk magnetic properties makes the high-dimensional

metal-azido systems of particular interest.^{15,16} In the neutral Cu-azido systems with chelating diamine ligands the dimensionalities are determined by the relative molar quantities of copper and the diamine ligand.^{17,18} Higher equivalent of the chelating ligand reduces the available sites on the metal for coordination by the bridging azido ligand and thus generally prefers lower dimensional structures. It has been also found from the literature that a simple change in the substitution on the diamine ligand dramatically changes the structure and magnetic behavior of the metal-azido systems.^{17,18} The change in the amount of the blocking diamine ligand should in principle change the structural pattern of Cu-azido systems. This prompted us to see the effect of systematic change in the amount of the blocking amine on the structural change of the Cu-azido systems. In our early work we have shown these effects with ethylenediamine.¹⁷ Here we report the synthesis, structural characterization, and variable temperature magnetic behavior of two new Cu-azido coordination polymers $[\text{Cu}_3(\text{N}_3)_6(\text{tmen})_2]_n$ (**1**) and $[\text{Cu}_6(\text{N}_3)_{12}(\text{deen})_2]_n$ (**2**) [$\text{tmen} = N,N,N',N'$ -tetramethylethylenediamine and $\text{deen} = N,N'$ -diethylethylenediamine]. **1** and **2** are one-dimensional (1D) and three-dimensional (3D) polymers of Cu_3 and Cu_6 secondary building clusters, respectively. Among the two, **1** is unique in the sense that it is the first polymeric Cu^{II} compound having a $[\text{Cu}(1,1-\text{N}_3)_2\text{Cu}]$ core with two $\text{Cu}-\text{N}_{\text{EO}}-\text{Cu}$ angles falling in both ferromagnetic and antiferromagnetic domain.

Experimental Section

Materials. $\text{Cu}(\text{NO}_3)_2 \cdot 3\text{H}_2\text{O}$, NaN_3 , N,N,N',N' -tetramethylethylenediamine (tmen), and N,N' -diethylethylenediamine (deen) were obtained from commercial sources and were used as received without further purification.

Physical Measurements. Elemental analyses of C, H, and N were performed using a Perkin-Elmer 240C elemental analyzer. IR spectra were recorded as KBr pellets using a Magna 750 FT-IR spectrophotometer. The measurements of variable-temperature magnetic susceptibility were carried out on a Quantum Design MPMS-XL5 SQUID magnetometer. Susceptibility data were collected using an external magnetic field of 0.05 T for **1** and at 0.2 T for **2** in the temperature range of 2 to 300 K. The experimental susceptibility data were corrected for diamagnetism (Pascal's tables).¹⁹

Caution! Although we did not experience any problems with the compounds reported in this work, azido complexes of metal ions in the presence of organic ligands are potentially explosive. Only a small amount of material should be prepared, and it should be handled with care.

(8) (a) Mukherjee, P. S.; Maji, T. K.; Mostafa, G.; Mallah, T.; Ray Chaudhuri, N. *Inorg. Chem.* **2000**, *39*, 5147. (b) Comarmond, J.; Plumere, P.; Lehn, J. M.; Agnus, Y.; Louis, R.; Weiss, R.; Kahn, O.; Morgesten-badarau, I. *J. Am. Chem. Soc.* **1982**, *104*, 6330. (c) Kahn, O.; Sikorav, S.; Gouteron, J.; Jeannin, S.; Jeannin, Y. *Inorg. Chem.* **1983**, *22*, 2877. (d) Tandon, S. S.; Thompson, L. K.; Manuel, M. E.; Bridson, J. N. *Inorg. Chem.* **1994**, *33*, 5555. (e) Ribas, J.; Monfort, M.; Ghosh, B. K.; Solans, X.; Font-Bardia, M. *J. Chem. Soc., Chem. Commun.* **1995**, 2375. (f) Ribas, J.; Monfort, M.; Ghosh, B. K.; Solans, X. *Angew. Chem., Int. Ed. Engl.* **1994**, *33*, 2177. (g) Viau, G.; Lambardi, G. M.; De Munno, G.; Julve, M.; Lloret, F.; Faus, J.; Caneschi, A.; Clemente-Juan, J. M. *Chem. Commun.* **1997**, 1195. (h) Escuer, A.; Vicente, R.; Ribas, J.; El Fallah, M. S.; Solans, X.; Font-Bardia, M. *Inorg. Chem.* **1993**, *32*, 3727. (i) Ruiz, E.; Cano, J.; Alvarez, S.; Alemany, P. *J. Am. Chem. Soc.* **1998**, *120*, 11122. (j) Aebbersold, M. A.; Gillon, M.; Plantevin, O.; Pardi, L.; Kahn, O.; Bergerat, I.; Seggern, V.; Ohstrom, L.; Grand, A.; Lelievre-Berna, E. *J. Am. Chem. Soc.* **1998**, *120*, 5238. (k) Shen, Z.; Zuo, J. -L.; Gao, S.; Song, Y.; Che, C. -M.; Fun, H. -K.; You, X. -Z. *Angew. Chem., Int. Ed.* **2000**, *39*, 3633. (l) Hong, C. S.; Koo, J.; Son, S. -K.; Lee, Y. S.; Kim, Y. -S.; Do, Y. *Chem.—Eur. J.* **2001**, *7*, 4243.

(9) Escuer, A.; Harding, C. J.; Dussart, Y.; Nelson, J.; McKee, V.; Vicente, R. *J. Chem. Soc., Dalton Trans.* **1999**, 223.

(10) Escuer, A.; Font-Bardí'a, M.; Massoud, S. S.; Mautner, F. A.; Peñalba, E.; Solans, X.; Vicente, R. *New J. Chem.* **2004**, *28*, 681.

(11) Hong, C. S.; Do, Y. *Angew. Chem., Int. Ed.* **1999**, *38*, 193.

(12) Mukherjee, P. S.; Dalai, S.; Zangrando, E.; Lloret, F.; Chaudhuri, N. R. *Chem. Commun.* **2001**, 1444.

(13) Saha, S.; Koner, S.; Tuchagues, J.-P.; Boudalis, A. K.; Okamoto, K. -I.; Banerjee, S.; Mal, D. *Inorg. Chem.* **2005**, *44*, 6379.

(14) Thompson, L. K.; Tandon, S. S.; Manuel, M. E. *Inorg. Chem.* **1995**, *34*, 2356.

(15) Mautner, F. A.; Hanna, S.; Cortés, R.; Lezama, L.; Barandika, M. G.; Rojo, T. *Inorg. Chem.* **1999**, *38*, 4647.

(16) Goher, M. A. S.; Cano, J.; Journaux, Y.; Abu-Youssef, M. A. M.; Mautner, F. A.; Escuer, A.; Vicente, R. *Chem.—Eur. J.* **2000**, *6*, 778.

(17) Mondal, K. C.; Mukherjee, P. S. *Inorg. Chem.* **2008**, *47*, 4215.

(18) (a) Gu, Z. -G.; Zuo, J. -L.; You, X. -Z. *Dalton Trans.* **2007**, 4067. (b) Gu, Z. -G.; Xu, Y. -F.; Yin, X. -J.; Zhou, X. -H.; Zuo, J. -L.; You, X. -Z. *Dalton Trans.* **2008**, 5593.

(19) (a) Dutta, R. L.; Syamal, A. *Elements of Magnetochemistry*, 2nd ed.; East West Press: Manhattan Beach, CA, 1993. (b) Kahn, O. *Molecular Magnetism*; VCH publisher: New York, 1993.

Table 1. Crystallographic Data and Refinement Parameters for **1** and **2**

	1	2
empirical formula	C ₁₂ H ₃₂ N ₂₂ Cu ₃	C ₁₂ H ₃₂ N ₄₀ Cu ₆
Fw	675.22	1118.02
T (K)	293 (2)	296 (2)
crystal system	monoclinic	monoclinic
space group	P2 ₁ /c	P2 ₁ /c
a/Å	8.5859(6)	8.9284(6)
b/Å	8.4242(6)	16.8024(12)
c/Å	18.4362(13)	13.0087(9)
α/deg	90.00	90.00
β/deg	96.587(1)	101.515(5)
γ/deg	90.00	90.00
V/Å ³	1324.68(16)	1912.3(2)
Z	2	4
ρ _{calcd} (g cm ⁻³)	1.693	1.942
μ (Mo Kα) (mm ⁻¹)	2.435	3.349
λ/Å	0.71073	0.71073
F(000)	690	944.6
collected reflns	10784	27871
unique reflns	3122	5834
GOF (F ²)	1.084	0.965
R ₁ ^a	0.0255	0.0588
wR ₂ ^b	0.0608	0.1890

$$^a R_1 = \sum ||F_o| - |F_c|| / \sum |F_o|. \quad ^b wR_2 = [\sum w(F_o^2 - F_c^2)^2 / \sum w(F_o^2)]^{1/2}.$$

Synthesis of Complex [Cu₃(N₃)₆(tmen)₂]_n (1**).** To a 10 mL methanolic solution of Cu(NO₃)₂·3H₂O (1.00 mmol, 241.6 mg) and tmen (0.67 mmol, 78 mg) an aqueous solution of NaN₃ (4.00 mmol, 260 mg) dissolved in minimum water was added slowly. The mixture was stirred for 5 min and filtered. Hexagonal black crystals of **1** were obtained in 24 h. Isolated Yield: 45%. Anal. Calcd for **1**, C₁₂H₃₂N₂₂Cu₃: C, 21.39; H, 4.79; N, 45.77. Found: C, 21.55; H, 4.93; N, 45.74. IR (KBr, cm⁻¹): 2057 and 2075 for the azido groups.

Synthesis of the Complex [Cu₆(N₃)₁₂(deen)₂]_n (2**).** To a 10 mL methanolic solution of Cu(NO₃)₂·3H₂O (1.00 mmol, 241.6 mg) and deen (0.25 mmol, 29 mg) was slowly added an aqueous solution of NaN₃ (4.00 mmol; 260 mg) dissolved in minimum water. The mixture was stirred for 2 min and filtered. Rectangular black crystals of **2** were obtained in 48 h. Isolated Yield: 30%. Anal. Calcd for **2**, C₁₂H₃₂N₄₀Cu₆: C, 12.93; H, 2.90; N, 50.28. Found: C, 13.02; H, 2.88; N, 50.20. IR (KBr, cm⁻¹): 2024, 2054, and 2089 for the azido groups.

X-ray Crystallographic Data Collection and Refinements. Single crystal X-ray data for **1** and **2** (Table 1) were collected on a Bruker SMART APEX CCD diffractometer using the SMART/SAINT software.²⁰ Intensity data were collected using graphite-monochromatized Mo Kα radiation (0.71073 Å) at 293 K. The structures were solved by direct methods using the SHELX-97²¹ program incorporated into WinGX.²² Empirical absorption corrections were applied with SADABS.²³ All non-hydrogen atoms were refined with anisotropic displacement coefficients. The hydrogen atoms bonded to carbon were included in geometric positions and given thermal parameters equivalent to 1.2 times those of the atom to which they were attached. Structures were drawn using ORTEP-3 for Windows.²⁴

(20) SMART/SAINT; Bruker AXS, Inc.: Madison, WI, 2004.

(21) Sheldrick, G. M. SHELX-97; University of Göttingen: Göttingen, Germany, 1998.

(22) Farrugia, L. J. *J. Appl. Crystallogr.* **1999**, *32*, 837. Farrugia, L. J. WinGX, version 1.65.04; Department of Chemistry, University of Glasgow: Glasgow, Scotland, 2003.

(23) Sheldrick, G. M. SADABS; University of Göttingen: Göttingen, Germany, 1999.

(24) ORTEP-3 for Windows, version 1.08; Farrugia, L. J. *J. Appl. Crystallogr.* **1997**, *30*, 565.

Computational Methodology

The exchange coupling constants in the reported linear complexes have been calculated using the following computational methodology.^{30–33} Using a phenomenological Heisenberg Hamiltonian $H = -\sum_i J_i S_i S_k$ (where i labels the different kinds of coupling constants, while j and k refer to the different paramagnetic centers) to describe the exchange coupling between each pair of transition-metal ions present in the polynuclear complex, the full Hamiltonian matrix for the entire system can be constructed.

To calculate the exchange coupling constants for any polynuclear complex with n different exchange constants, at least the energy of $n + 1$ spin configurations must be calculated. In the case of the studied trinuclear complexes, the exchange coupling value J was obtained by taking into account the energy of two different spin distributions: high spin quartet (Q) with $S = 3/2$ and low spin doublet with $S = 1/2$. The following equation has been employed to calculate the exchange coupling constant,

$$J = 2\Delta E/S(S + 1), \quad \Delta E = E_{D(BS)} - E_Q$$

The hybrid B3LYP functional³⁴ has been used in all calculations as implemented in the Gaussian 03 package,³⁵ mixing the exact Hartree–Fock-type exchange with Becke's expression for the exchange functional³⁶ and that proposed by Lee–Yang–Parr for the correlation contribution.³⁷ The use of the nonprojected energy of the broken-symmetry solution as the energy of the low spin state within the DFT framework provides more or less satisfactory results avoiding the cancellation of the nondynamic correlation effects.³⁸ The broken symmetry approach along with electron correlations at the B3LYP level has been widely used to investigate magnetic properties in a large number of magnetic systems.

(25) Escuer, A.; Goher, M. A. S.; Mautner, F. A.; Vicente, R. *Inorg. Chem.* **2000**, *39*, 2107.

(26) Song, Y.; Massera, C.; Quesada, M.; Manotti Lanfredi, A. M.; Mutikainen, I.; Turpeinen, U.; Reedijk, J. *Inorg. Chim. Acta* **2005**, *358*, 1171.

(27) Lam, M. H. W.; Tang, Y.-T.; You, X.-Z.; Wong, W.-T. *Chem. Commun.* **1997**, 957.

(28) Luo, J.; Zhou, X.-G.; Gao, S.; Weng, L.-H.; Shao, Z.-H.; Zhang, C.-M.; Li, Y.-R.; Zhang, J.; Cai, R.-F. *Polyhedron* **2004**, *23*, 1243.

(29) Stamatatos, T. C.; Papaefstathiou, G. S.; MacGillivray, L. R.; Escuer, A.; Vicente, R.; Ruiz, E.; Perlepes, S. P. *Inorg. Chem.* **2007**, *46*, 8843.

(30) Ruiz, E.; Alemany, P.; Alvarez, S.; Cano, J. *J. Am. Chem. Soc.* **1997**, *119*, 1297.

(31) Ruiz, E.; Rodríguez-Fortea, A.; Cano, J.; Alvarez, S.; Alemany, P. *J. Comput. Chem.* **2003**, *24*, 982.

(32) Ruiz, E.; Cano, J.; Alvarez, S.; Alemany, P. *J. Comput. Chem.* **1999**, *20*, 1391.

(33) Ruiz, E. *Struct. Bonding (Berlin)* **2004**, *113*, 71.

(34) Becke, A. D. *J. Chem. Phys.* **1993**, *98*, 5648.

(35) Frisch, M. J.; Trucks, G. W.; Schlegel, H. B.; Scuseria, G. E.; Robb, M. A.; Cheeseman, J. R.; Montgomery, J. A.; Vreven, T.; Kudin, K. N.; Burant, J. C.; Millam, J. M.; Iyengar, S. S.; Tomasi, J.; Barone, V.; Mennucci, B.; Cossi, M.; Scalmani, G.; Rega, N.; Petersson, G. A.; Nakatsuji, H.; Hada, M.; Ehara, M.; Toyota, K.; Fukuda, R.; Hasegawa, J.; Ishida, H.; Nakajima, T.; Honda, Y.; Kitao, O.; Nakai, H.; Klene, M.; Li, X.; Knox, J. E.; Hratchian, H. P.; Cross, J. B.; Adamo, C.; Jaramillo, J.; Gomperts, R.; Stratmann, R. E.; Yazyev, O.; Austin, A. J.; Cammi, R.; Pomelli, C.; Ochterski, J.; Ayala, P. Y.; Morokuma, K.; Voth, G. A.; Salvador, P.; Dannenberg, J. J.; Zakrzewski, V. G.; Dapprich, S.; Daniels, A. D.; Strain, M. C.; Farkas, O.; Malick, D. K.; Rabuck, A. D.; Raghavachari, K.; Foresman, J. B.; Ortiz, J. V.; Cui, Q.; Baboul, A. G.; Clifford, S.; Cioslowski, J.; Stefanov, B. B.; Liu, G.; Liashenko, A.; Piskorz, P.; Komaromi, I.; Martin, R. L.; Fox, D. J.; Keith, T.; Al-Laham, M. A.; Peng, C. Y.; Nanayakkara, A.; Challacombe, M.; Gill, P. M. W.; Johnson, B.; Chen, W.; Wong, M. W.; Gonzalez, C.; Pople, J. A. *Gaussian 03*, revision B.4; Gaussian Inc.: Pittsburgh, PA, 2003.

(36) Becke, A. D. *Phys. Rev. A* **1988**, *38*, 3098.

(37) Lee, C.; Yang, W.; Parr, R. G. *Phys. Rev. B* **1988**, *37*, 785.

(38) Ruiz, E.; Alvarez, S.; Cano, J.; Polo, V. *J. Chem. Phys.* **2005**, *123*, 164110.

We have considered LANL2DZ basis set for Cu and 6-31G for rest of the atoms. All of the energy calculations were performed including a 10^{-8} density-based convergence criterion.

Results and Discussion

Synthesis. Both the complexes were obtained from the reaction of $\text{Cu}(\text{NO}_3)_2 \cdot 3\text{H}_2\text{O}$ and lower molar equivalents

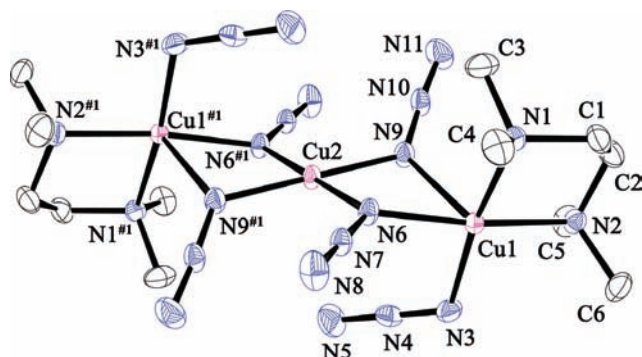


Figure 1. ORTEP view of the basic unit of **1**. Hydrogen atoms have been removed for clarity. Thermal ellipsoids are at 30% probability level.

of chelating diamine ligands with excess of NaN_3 in a $\text{MeOH}/\text{H}_2\text{O}$ mixture. When excess of NaN_3 is used it normally prevents the immediate precipitation and allows the formation of multidimensional compounds via self-assembly of the smaller units. Intense and broad infrared absorptions of azido stretching vibrations at 2057 and 2075 cm^{-1} for **1**, and 2024, 2054, and 2089 cm^{-1} for **2**, respectively, are consistent with the presence of various bonding modes of the bridging azido ligands.

Structure Description of $[\text{Cu}_3(\text{N}_3)_6(\text{tmen})_2]_n$ (1**).** It is a centrosymmetric trinuclear complex (Figure 1). Important interatomic distances and angles are given in Table 2. The coordination geometry around the central Cu(2) ion, which sits on the inversion center, is square planar and is linked to two Cu(1) ions through four $\mu_{1,1}$ -azido ligands. Each of the two terminal Cu(1) atoms adopt a square-pyramidal geometry with one $\mu_{1,1}$ -azide ligand, two nitrogen atoms of the chelating tmen ligand, and a terminal azide ligand forming the basal plane and another $\mu_{1,1}$ -azide ligand at the apical position. The adjacent Cu atoms are at a distance of about 3.26 Å. The four short basal bonds of the terminal Cu(1) atoms range from 1.9810(17) to 2.0698(15) Å and the longer axial Cu(1)–N(9) bond

Table 2. Selected Bond Distances (Å) and Angles (deg) for **1** and **2**^a

1, Bond Distances (Å)					
Cu(1)–N(1)	2.0698(15)	Cu(1)–N(2)	2.0442(16)	Cu(1)–N(3)	1.9810(17)
Cu(1)–N(6)	2.0222(15)	Cu(1)–N(9)	2.505(1)	Cu(1)–N(8)	2.817(1)
Cu(2)–N(6)	2.0028(15)	Cu(2)–N(6) ^{#1}	2.0028(15)	Cu(2)–N(9)	1.9733(16)
Cu(2)–N(9) ^{#1}	1.9733(16)	N(7)–N(6)	1.209(2)	N(4)–N(5)	1.164(3)
N(10)–N(11)	1.153(3)	N(10)–N(9)	1.195(2)	N(4)–N(3)	1.187(2)
N(7)–N(8)	1.139(2)				
1, Bond Angles (deg)					
N(9) ^{#1} –Cu(2)–N(9)	180.00	N(9) ^{#1} –Cu(2)–N(6) ^{#1}	95.55(7)		
N(9)–Cu(2)–N(6) ^{#1}	84.45(7)	N(6) ^{#1} –Cu(2)–N(6)	180.00		
N(3)–Cu(1)–N(6)	92.22(7)	N(3)–Cu(1)–N(2)	91.19(7)		
N(6)–Cu(1)–N(2)	172.12(7)	N(3)–Cu(1)–N(1)	169.89(7)		
N(6)–Cu(1)–N(1)	91.80(7)	N(2)–Cu(1)–N(1)	86.02(7)		
Cu(2)–N(6)–Cu(1)	108.25(7)	Cu(2)–N(9)–Cu(1)	92.72(2)		
N(7)–N(6)–Cu(2)	124.10(12)	N(10)–N(9)–Cu(2)	127.24(15)		
N(4)–N(3)–Cu(1)	116.66(14)	N(7)–N(6)–Cu(1)	124.68(13)		
2, Bond Distances (Å)					
Cu(2)–N(15)	1.983(5)	Cu(2)–N(6)	1.985(6)	Cu(2)–N(12)	2.024(5)
Cu(2)–N(3)	2.025(5)	Cu(2)–N(18)	2.465(8)	Cu(1)–N(1)	2.019(7)
Cu(1)–N(2)	2.021(6)	Cu(1)–N(9)	2.027(5)	Cu(1)–N(6)	2.029(6)
Cu(1)–N(3)	2.602(2)	Cu(1)–N(5)	2.494(3)	Cu(3)–N(3)	2.548(1)
Cu(3)–N(20)	1.948(6)	Cu(3)–N(9)	1.999(5)	Cu(3)–N(15)	2.011(5)
Cu(3)–N(12)	2.023(5)	N(6)–N(7)	1.207(8)	N(7)–N(8)	1.137(9)
N(9)–N(10)	1.183(7)	N(10)–N(11)	1.138(8)	N(15)–N(16)	1.212(8)
N(16)–N(17)	1.139(9)	N(12)–N(13)	1.214(9)	N(13)–N(14)	1.164(9)
N(3)–N(4)	1.191(7)	N(4)–N(5)	1.137(8)	N(18)–N(19)	1.165(8)
N(19)–N(20)	1.197(8)				
2, Bond Angles (deg)					
N(15)–Cu(2)–N(6)	165.0(2)	N(15)–Cu(2)–N(18) ^{#2}	103.9(3)		
N(6)–Cu(2)–N(12)	98.0(2)	N(12)–Cu(2)–N(18) ^{#2}	96.3(2)		
N(2)–Cu(1)–N(6)	160.8(3)	N(9)–Cu(1)–N(6)	90.5(2)		
N(1)–Cu(1)–N(2)	85.5(3)	N(2)–Cu(1)–N(9)	93.1(3)		
N(20)–Cu(3)–N(15)	170.5(3)	N(9)–Cu(3)–N(15) ^{#3}	93.4(2)		
N(9)–Cu(3)–N(12) ^{#3}	171.6(2)	N(15)–Cu(3)–N(12)	78.4(2)		
Cu(1)–N(6)–Cu(2)	109.55(2)	Cu(1)–N(9)–Cu(3)	114.10(1)		
Cu(1)–N(3)–Cu(2)	89.36(3)	Cu(1)–N(3)–Cu(3)	81.98(2)		
Cu(2)–N(12)–Cu(3)	100.30(2)	Cu(2)–N(15)–Cu(3)	102.16(3)		

^a Symmetry transformations used to generate equivalent atoms: #1 $-x+1, -y+1, -z+2$; #2 $x-1, y, z$; #3 $-x, -y, -z+1$.

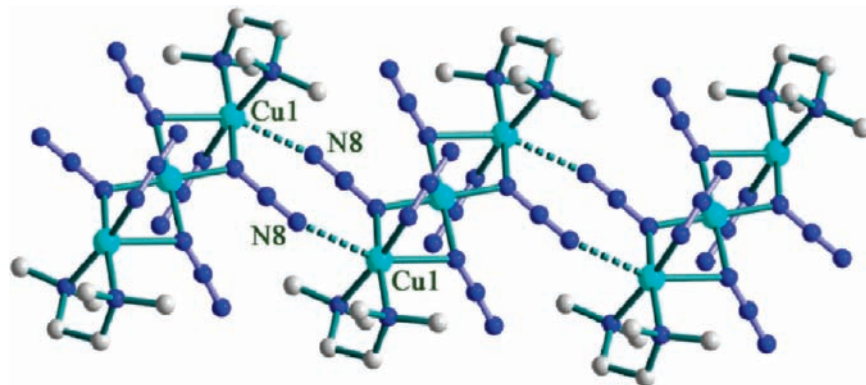
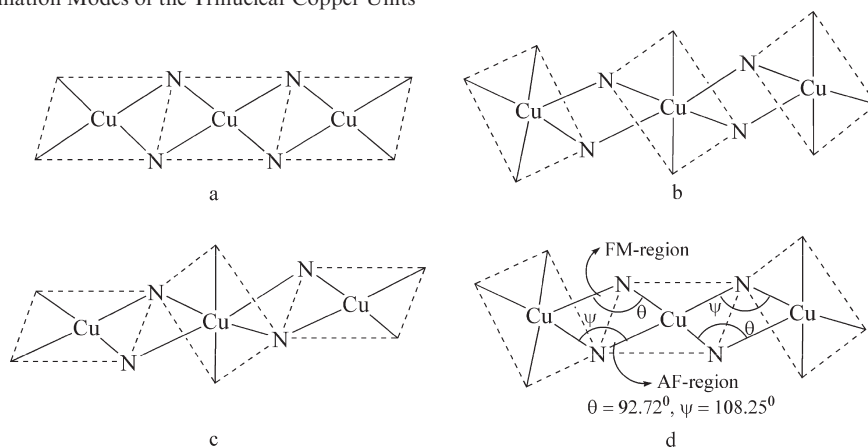


Figure 2. Ball and stick representation of the 1D arrangement of **1**.

Chart 1. Various Coordination Modes of the Trinuclear Copper Units



measures at 2.505(1) Å. Cu(2) has two sets of symmetrical bonds with adjacent azido-N atoms (Cu(2)–N(6), 2.0028(15) Å; Cu(2)–N(9), 1.9733(16) Å). There are two more nitrogen atoms [N(5)] on the axial positions of Cu(2), but too far (~2.9 Å) for the Cu–N distance to be considered even as an axially elongated bond. Similarly there is one more nitrogen atom [N(8)] at the sixth coordination positions of the terminal Cu(1) atoms at a distance of 2.817(1) Å opposite to the axial N(9) atom. If we consider this as a bonding interaction between Cu(1) and N(8) then **1** becomes a 1D polymer of the basic trinuclear unit connected by two $\mu_{1,1,3}$ -azido bridges (Figure 2).

The $[\text{Cu}(\mu_{1,1}\text{-N}_3)_2\text{Cu}]^{2+}$ core in **1** is irregularly asymmetric (part d of Chart 1) with three short bonds and one long bond. To the best of our knowledge, there are five other structurally characterized Cu^{II} complexes known in literature that have a related trinuclear unit. Three of them, namely, $[\text{Cu}_3(\text{N}_3)_6(\text{Meinic})_2(\text{DMF})_2]_n$,²⁵ $[\text{Cu}_3(\text{N}_3)_6(\text{ampym})_2(\text{DMF})_2]_n$,²⁶ and $[\text{Cu}_3(\text{N}_3)_6\text{L}_2]^{27}$ [where Meinic = methylisonicotinate, ampym = 2-aminopyrimidine, and L = hydridotris(3,5-dimethylpyrazolyl)borate] have a symmetric trinuclear unit (part 'a' of Chart 1); $[\text{Cu}_3(\text{N}_3)_6(\text{det})_2]^{28}$ has an asymmetric unit as shown in part 'b' of Chart-1 and another complex $[\text{Cu}_3(\text{N}_3)_6(2,2\text{-tpcb})\text{-}(\text{DMF})_2]_n$ ²⁹ has an irregular trinuclear asymmetric unit (part 'c' of Chart 1). For the first four complexes, the two Cu–N_{EO}–Cu angles within the core $[\text{Cu}(\mu_{1,1}\text{-N}_3)_2\text{Cu}]^{2+}$ are very close to each other (within 2°). The last complex, however, has two angles widely separated (105.39° and 89.76°) just like complex **1** (108.25° and 92.72°) though

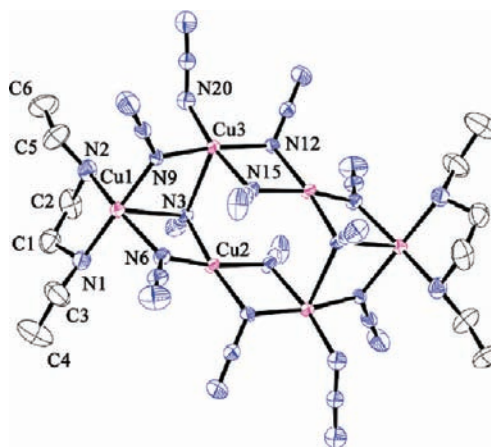


Figure 3. ORTEP view of the basic unit of **2**. Hydrogen atoms have been removed for the sake clarity. Thermal ellipsoids are at 30% probability level.

both the angles fall in the ferromagnetic region. But complex **1** (part 'd' of Chart 1) is the only one in this series having these angles on both sides of the critical magnetic exchange angle of 108°.

Structure Description of $[\text{Cu}_6(\text{N}_3)_{12}(\text{deen})_2]_n$ (2**).** Complex **2** is a complicated 3D coordination assembly of hexanuclear copper(II) cluster $[\text{Cu}_6(\text{N}_3)_{12}(\text{deen})_2]$ connected by azido bridges. The repeating building unit contains six Cu(II) ions arranged in sandwich-like layers of three, that are linked together by 10 EO bridging azido groups (Figure 3). The copper atoms coordinated to the

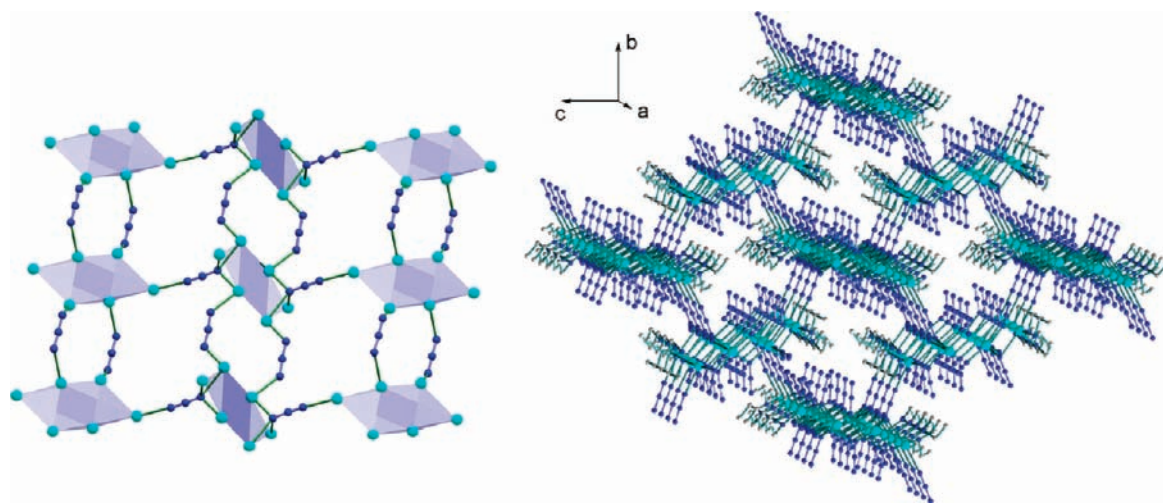


Figure 4. View of the 2D units in the structure of **2** (left) and ball and stick representation of the 3D arrangement of **2** (right).

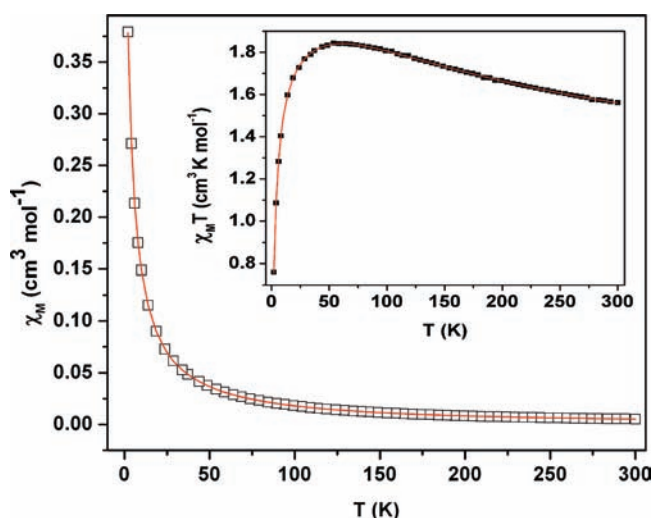


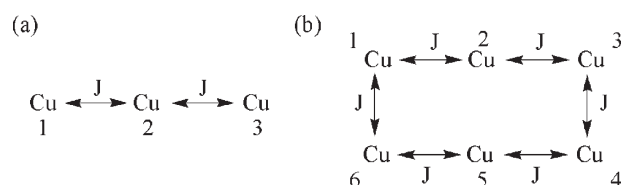
Figure 5. Plots of χ_M versus T and $\chi_M T$ versus T (inset) for complex **1** in the temperature range of 2–300 K. The red line indicates the fitting using theoretical model (see text).

deen ligands are in an elongated octahedral environment [$\text{Cu}-\text{N}_{\text{eq}}$, 2.019(7)–2.029(6) Å; $\text{Cu}-\text{N}_{\text{ax}}$, 2.494(3) and 2.602(2) Å] and the other copper atoms assume square-pyramidal geometry completed by five azido ligands [$\text{Cu}-\text{N}_{\text{basal}}$, 1.983(5)–2.025(5) Å; $\text{Cu}-\text{N}_{\text{apical}}$, 2.465(8)–2.548(1) Å]. Within the basic Cu^{II}_6 unit, the $\text{Cu}-\text{N}_{\text{EO}}-\text{Cu}$ angles are distributed within the range 81.98° to 114.10°. The intracluster adjacent Cu–Cu distances are within the range of 3.107–3.378 Å. Each Cu^{II}_6 unit is joined with two neighboring such units through double $\mu_{1,3}$ (EE) azido bridges along a axis and with other four units through single $\mu_{1,1,1,3}$ azido ligands parallel to the bc plane to yield a 3D network (Figure 4). By ascribing the Cu^{II}_6 clusters as nodes and the azido ligands as linkers the 3D framework can be justified as a primitive cubic net.

Magnetic Behavior

Complex 1. The plots of both χ_M versus T and $\chi_M T$ versus T for **1** per Cu^{II}_3 unit are shown in Figure 5. The room temperature (300 K) $\chi_M T$ value of 1.56 $\text{cm}^3 \text{K mol}^{-1}$ is slightly higher than the three uncoupled Cu^{II} ions ($\chi_M T = 0.375 \text{ cm}^3 \text{K mol}^{-1}$ for an $S = 1/2$ ion). The $\chi_M T$ value

Scheme 2. Schematic Diagrams Representing the Exchange Interactions within (a) Complex **1** and (b) Complex **2**



gradually increases upon decreasing temperature from 300 K and reaches a maximum value of 1.84 $\text{cm}^3 \text{K mol}^{-1}$ at 54 K. Further cooling decreases the $\chi_M T$ value to 0.75 $\text{cm}^3 \text{K mol}^{-1}$ at 2 K. The $1/\chi_M$ versus T plot (300–50 K) obeys the Curie–Weiss law with a positive Weiss constant of $\theta = 16.03$ K. The nature of the $\chi_M T$ versus T plot and the positive θ suggest a dominant ferromagnetic exchange among the three Cu^{II} ions through azido bridges.

From the structural point of view for this centrosymmetric complex, the two EO-azido bridges between $\text{Cu}(2)$ and two $\text{Cu}(1)$ ion on both sides account for the magnetic exchange pathway. Symmetry makes the two exchange parameters to be the same (Scheme 2). A reasonable fit can be obtained for interacting trinuclear units applying the conventional Hamiltonian:

$$H = -J(S_1 S_2 + S_2 S_3)$$

introducing an intertrimer zJ' term. Considering these two different exchange parameters, the analysis of the experimental susceptibility values has been performed using the following expression:

$$\chi_M = \chi_M' / \{1 - \chi_M'(2zJ'/Ng^2\beta^2)\} + \alpha_{\text{TIP}}$$

$$\chi_M' = (Ng^2\beta^2/3kT)[A/B]$$

where $A = [15 \exp(3J/2kT) + (3/2) \exp(J/kT) + (3/2)]$ and $B = [4 \exp(3J/2kT) + 2 \exp(J/kT) + 2]$.

The values giving the best fit (2–300 K) are $J = +262.12 \text{ cm}^{-1}$, $zJ' = -0.89 \text{ cm}^{-1}$, $g = 2.04$ and $\alpha_{\text{TIP}} = 0.0013 \text{ cm}^3 \text{mol}^{-1}$ ($R = 3.2 \times 10^{-5}$).

It is well-known in the literature that in EO-bridged Cu-azido systems the $\text{Cu}-\text{N}_{\text{EO}}-\text{Cu}$ angle plays a vital role in

determining the nature of magnetic exchange between the metal ions. Smaller angles ($< 108^\circ$) favor ferromagnetic and larger angles ($> 108^\circ$) favor antiferromagnetic exchange. Now in **1** any two adjacent Cu ions are linked

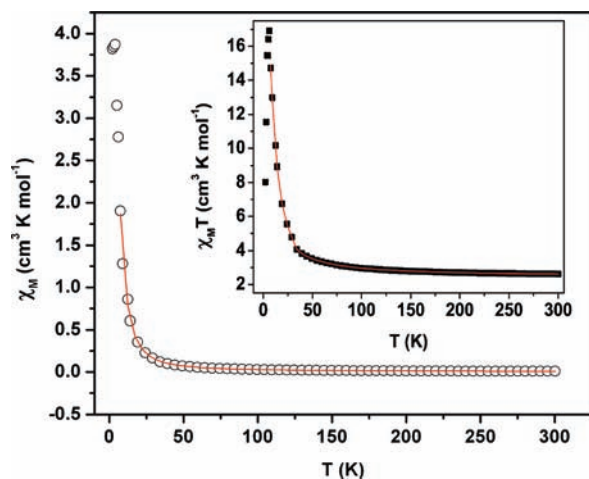


Figure 6. Plots of χ_M versus T and $\chi_M T$ versus T (inset) for complex **2** in the temperature range of 2–300 K. The red line indicates the fitting using theoretical model (see text).

by two non-identical EO-azido ligands with very different bridging Cu–N_{EO}–Cu angles [Cu(1)–N(9)–Cu(2) = 92.72° and Cu(2)–N(6)–Cu(1) = 108.25°]. The short angle bridge is asymmetric with short (equatorial) and long (axial) Cu–N bonds (1.97 and 2.51 Å). So **1** is a unique trinuclear complex having two bridging azides with the Cu–N_{EO}–Cu angles in both ferromagnetic (F-azido) and antiferromagnetic (AF-azido) domains. Experiment shows that the overall exchange is in fact ferromagnetic and that the intertrimer interaction is very weak and is antiferromagnetic.

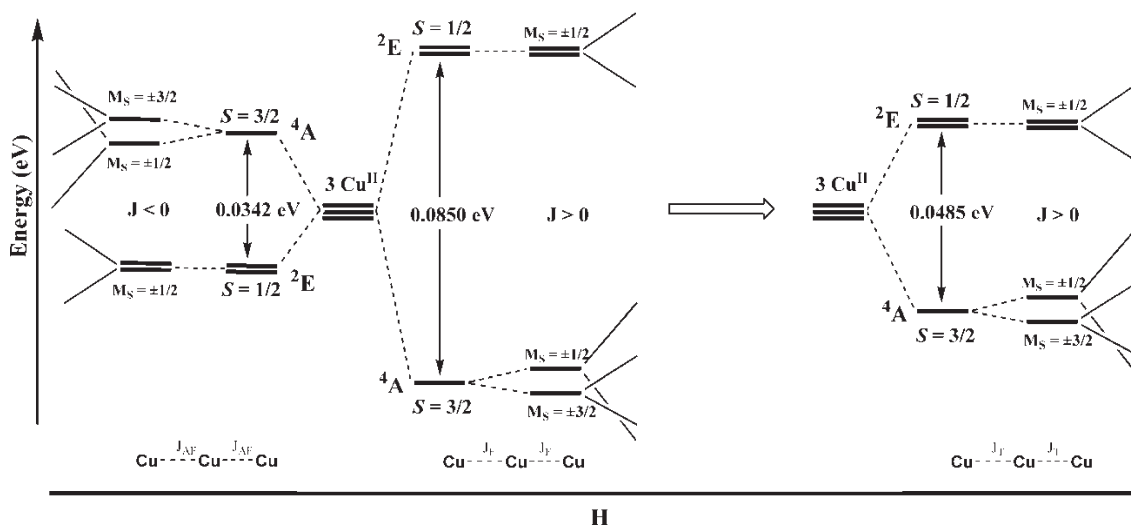
Complex 2. Figure 6 shows the temperature dependence of χ_M and $\chi_M T$ values for complex **2**. At room temperature $\chi_M T = 2.61 \text{ cm}^3 \text{ K mol}^{-1}$ and is a little

Table 3. Summary of DFT Calculations for Complex **1**^{a,b}

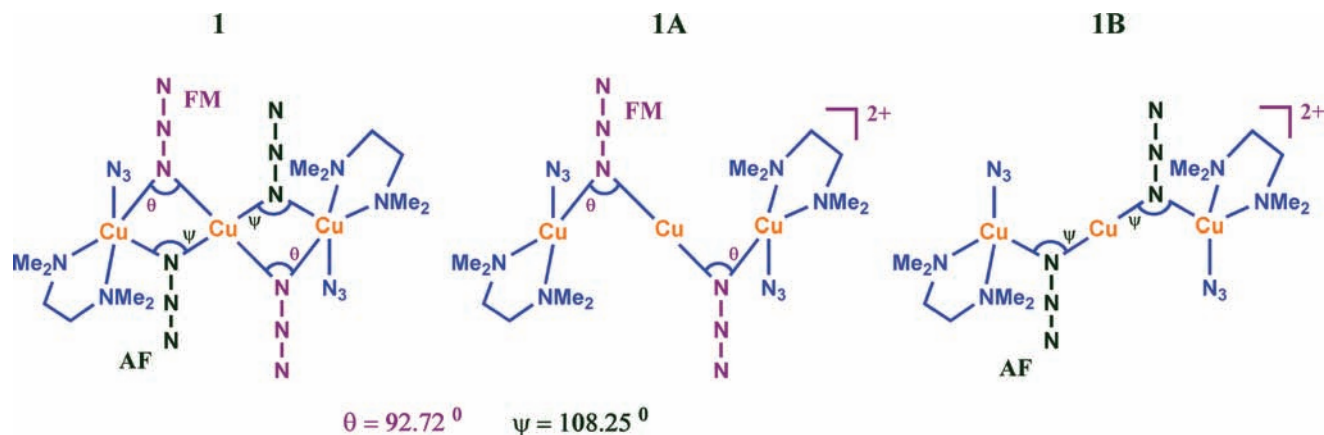
system	$\Delta E = E_{D(\text{BS})} - E_Q \text{ cm}^{-1}$	$J = 2\Delta E / [S(S+1)] \text{ cm}^{-1}$
(1) original molecule	391.45	208.78 (J_T)
(1A) two AF azido removed	685.51	365.60 (J_F)
(1B) two FM azido removed	-276.16	-147.29 (J_{AF})

^a Experimental resultant J value for **1** is 281.79 cm^{-1} . ^b $J_F + J_{AF} = (365.60 - 147.29) \text{ cm}^{-1} = 218.31 \text{ cm}^{-1} \approx J_T = 208.78 \text{ cm}^{-1}$.

Scheme 3. Energy Diagram of Ferromagnetically (**1** and **1A**) and Antiferromagnetically (**1B**) Coupled Linear Tricopper Units



Scheme 4. Systems Used for Computational Studies



higher than expected for six uncoupled Cu^{II} ions. The $\chi_{\text{M}}T$ value gradually increases upon decreasing temperature, but a sudden jump is observed below 25 K, giving a maximum value of $16.90 \text{ cm}^3 \text{ K mol}^{-1}$ at 6 K. Further cooling decreases the $\chi_{\text{M}}T$ value to $8.02 \text{ cm}^3 \text{ K mol}^{-1}$ at 2 K. The $1/\chi_{\text{M}}$ versus T plot (300–20 K) obeys the Curie–Weiss law with a positive Weiss constant of $\theta = 15.09 \text{ K}$. The nature of the $\chi_{\text{M}}T$ versus T

plot and the positive θ suggest a dominant ferromagnetic exchange among the six Cu^{II} ions through azido bridges.

Assuming the exchange pathways in the basic Cu^{II}_6 units (Scheme 2) to be uniform, a reasonable fit is obtained applying the Hamiltonian

$$H = -J(S_1S_2 + S_2S_3 + S_3S_4 + S_4S_5 + S_5S_6 + S_6S_1)$$

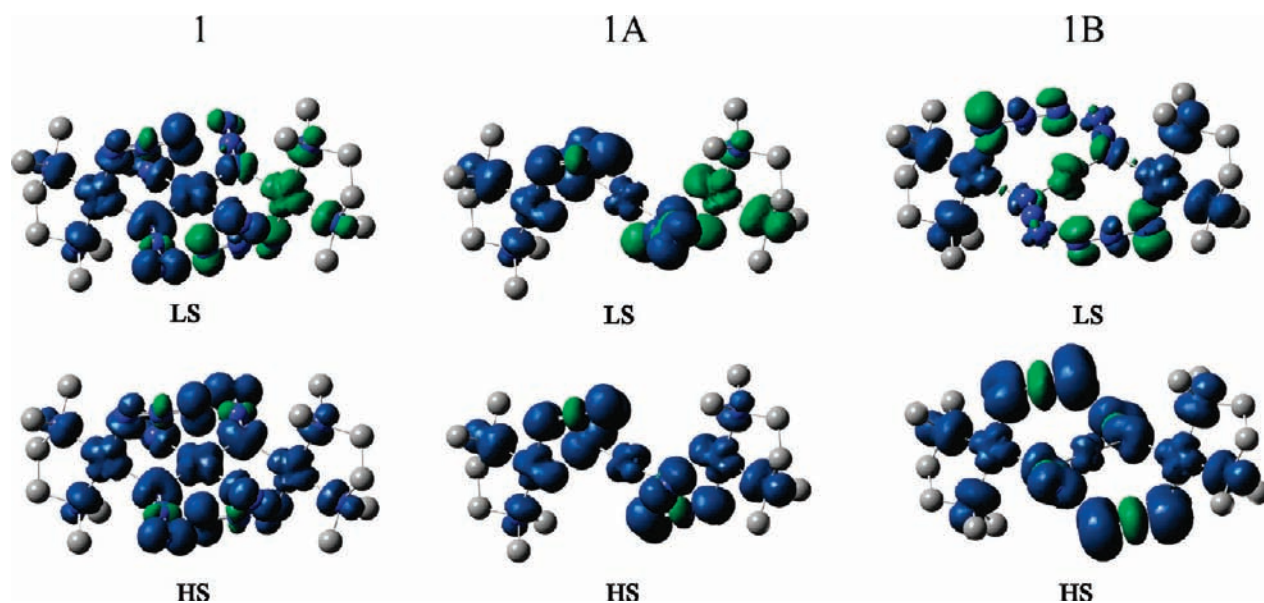


Figure 7. Spin density maps calculated for **1**, **1A**, and **1B** at B3LYP level for a single-determinant corresponding to their LS doublet and HS quartet states. Positive and negative spin populations are represented as blue and green surfaces. The isodensity surfaces correspond to a value of 0.0025 e/b^3 .

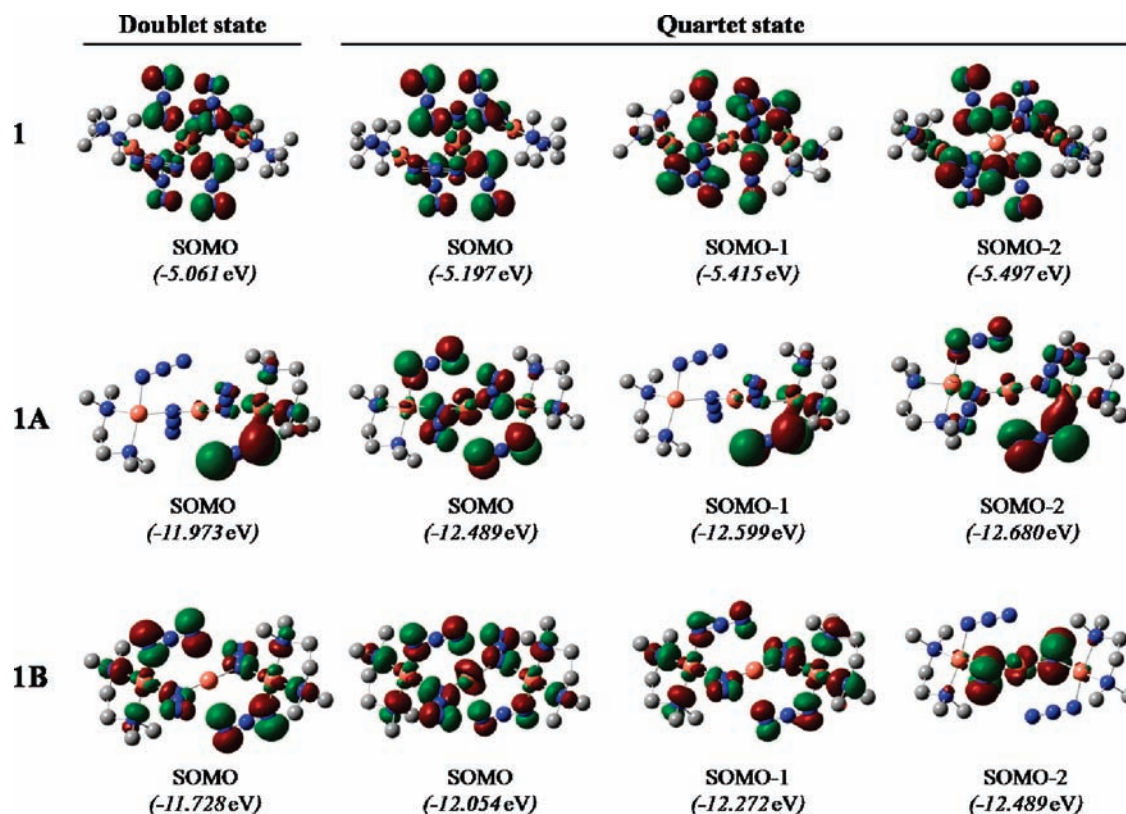


Figure 8. Bonding and antibonding combinations of the SOMOs of **1**, **1A**, and **1B**.

Table 4. Atomic Spin Densities (in au) of **1**, **1A**, and **1B** in Both Their Low Spin Doublet and the High Spin Quartet States

atom	1		1A		1B	
	LS	HS	LS	HS	LS	HS
Cu(1)	0.493	0.481	0.130	0.118	-0.089	0.042
Cu(1')	-0.512	0.481	0.425	0.437	0.378	0.430
Cu(2)	0.517	0.507	-0.412	0.441	0.380	0.434
N(6)	0.119	0.121			-0.005	0.101
N(6')	-0.008	0.119			0.004	-0.036
N(9)	0.067	0.076	0.227	0.199		
N(9')	0.072	0.076	0.236	0.177		

and introducing an intercluster zJ' term. Considering the two different exchange parameters, the analysis of the experimental susceptibility values has been performed using the following expression:

$$\chi_M = \chi_M' / \{1 - \chi_M'(2zJ'/Ng^2\beta^2)\} + \alpha_{(\text{TIP})}$$

$$\chi_M' = (Ng^2\beta^2/kT)[A/B]$$

where $A = 14 + 9 \exp(-5J/kT) + 25 \exp(-3J/kT)$ and $B = 7 + 27 \exp(-5J/kT) + 5 \exp(-6J/kT) + 25 \exp(-3J/kT)$. The values giving the best fit (7–300 K) are $J = 9.05 \text{ cm}^{-1}$, $zJ' = -0.85 \text{ cm}^{-1}$, $g = 2.06$, and $\alpha_{(\text{TIP})} = 0.0049 \text{ cm}^3 \text{ mol}^{-1}$ ($R = 6.8 \times 10^{-5}$). So the exchange interaction between the clusters is weakly antiferromagnetic. Fitting below 7 K was not satisfactory, which could be due to complex intermolecular interactions.

Theoretical Study. To examine and understand the above results in the reported compounds, DFT calculations were performed using the atomic coordinates as obtained from the single crystal X-ray structures. The interesting features regarding the two Cu–N_{EO}–Cu bridging angles in complex **1** provides an opportunity to probe the magnetic exchange coupling mechanism through theoretical calculations. Apart from the bridging angles, the Cu–N(bridge) distances, the Cu···Cu separation, and the geometries around the metal center can also influence the coupling, though the effects are often very small and negligible. Our main focus was to investigate the effects of the two kinds of bridging azido groups separately. The magnetic exchange interaction in a linear arrangement of three $S = 1/2$ ions results in two electronic states, that is, a doubly degenerate doublet ($S = 1/2$, 2E) and a quartet state ($S = 3/2$, 4A). Depending upon the relative energies of these states the complex may become antiferromagnetic or ferromagnetic (Scheme 3). The magnetic exchange parameter J can be calculated from this relative energy difference by using density functional methods. The exchange coupling parameter J value depends upon the relative energies of the doublet and quartet states. So, we assumed that a good approximation can be obtained for the contribution of the two kinds of EO-azido groups (AF-azido and F-azido) to the overall exchange parameter, if we selectively remove the AF-azido and F-azido groups and estimate the J values for the two resulting dicationic species (**1A** and **1B**) (Scheme 4).²⁹

The results of the DFT calculations have been summarized in Table 3. The estimated magnetic exchange constant (J_T) for **1**, though low, is quite consistent with the experimental ferromagnetic behavior.

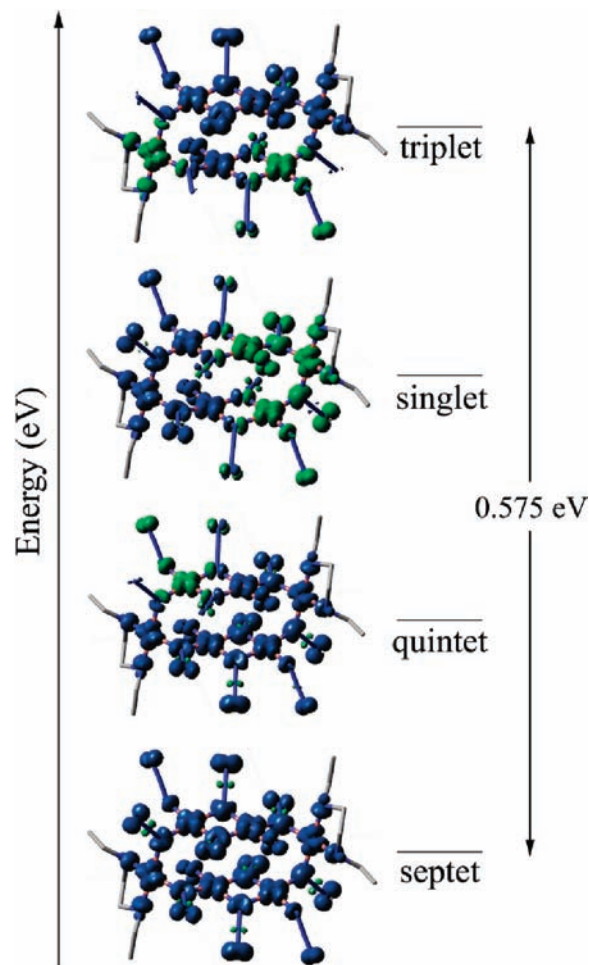


Figure 9. Spin density maps calculated for **2** at B3LYP level for single-determinant corresponding to the singlet, triplet, quintet, and septet states. Positive and negative spin populations are represented as blue and green surfaces. The isodensity surfaces correspond to a value of 0.0025 e/b^3 .

The fictitious species **1A** gives a very high positive value for the exchange constant ($J_F = 365.60 \text{ cm}^{-1}$), as is expected for an EO-azido bridged system with Cu–N_{EO}–Cu angle well below the critical value. Similarly, the species **1B** with only the two AF-azido bridges gives a moderately negative value for the exchange parameter ($J_{AF} = -147.29 \text{ cm}^{-1}$). The two individual contributions (J_F and J_{AF}) roughly adds up to make the overall exchange constant to be moderately positive and this consistency ($J_F + J_{AF} \approx J_T$) also provides support for our approach of selective elimination of the azido groups.

The representation of the spin distribution corresponding to the quartet and doublet states for **1**, **1A**, and **1B** are plotted in Figure 7, and the atomic spin densities of the three Cu^{II} atoms and the bridging N atoms of the two states are summarized in Table 4. For all the three systems the orientation of the orbitals possessing the unpaired electrons between the neighboring Cu^{II} atoms is orthogonal to each other. The ground states of complex **1** and **1A** show that the atoms with large spin densities have the same sign. For **1B**, it is the excited state that has a similar spin distribution.

The influence of the different EO-azido groups, as well as the coordination spheres of the Cu^{II} atoms in **1** and its

two fictitious analogues **1A** and **1B**, can be clearly envisaged from the plots of the singly occupied molecular orbitals (SOMOs) of their two states (Figure 8). A very weak antiferromagnetic contribution is expected in **1** and **1A**, as the central copper atom shows highly localized molecular orbitals at higher energies, not favoring mixing with the orbitals of the other two copper atoms.

The J value obtained from the DFT calculations for complex **2** is high (347.88 cm^{-1}) compared to the experimentally fitted one, because the DFT calculation was done on a Cu^{II}_6 unit while the fitting of the experimental data was done considering intercluster interaction. The calculation, however, predicts the ground state to be the high-spin septet state supporting ferromagnetic exchange between the Cu^{II} ions. The spin density plots for all the four possible states are given in Figure 9 in order of their calculated energies. It can be noted that the energy order of the singlet and the triplet states are reversed. The spin densities of the six Cu^{II} atoms and the ten bridging N atoms are compiled in Table S1 (Supporting Information). The ground state can be seen to have large spin densities on the atoms with the same sign, as expected for a ferromagnetic complex.

Concluding Remarks

The structures and magnetic properties along with some theoretical (DFT) analysis are reported for two new copper-

azido polymers. These complexes were prepared with a view that decreasing the molar amount of blocking diamine ligands opens more sites for the bridging azido ligand to link. Both the complexes were found to be predominantly ferromagnetic in nature. Though several polynuclear metal azido complexes are known with both ferromagnetic and antiferromagnetic pathways, complex **1** represents the first example of a Cu-azido polymer having $[\text{Cu}(\text{N}_3)_2\text{Cu}]$ magnetic core with Cu–N–Cu angles in both ferromagnetic and antiferromagnetic regions. Overall experimental magnetic behavior in both the complexes was corroborated with DFT calculations. Use of blocking amine ligand in less than one equivalent with respect to the metal in conjunction with azido and other pseudo halides and formation variety of assemblies with interesting structures and properties has the potential to considerably expand this methodology.

Acknowledgment. S.M. gratefully acknowledges the Council of Scientific and Industrial Research, New Delhi, India for the award of a Research Fellowship. The authors also thank the Department of Science and Technology (DST), New Delhi for financial support.

Supporting Information Available: X-ray crystallographic data in CIF format, Curie–Weiss fitting of the χ_M^{-1} versus T data of **1** and **2** and atomic spin densities of complex **2**. This material is available free of charge via the Internet at <http://pubs.acs.org>.